Optimizing Turbidity Removal Using Leaf-Based Natural Coagulants: Influence of pH, Dosage, and Settling Time

Saad M. Hasan[a*], Asia Fadhile Almansoory[b] Israa Abdulwahab Al-Baldawi[c]

a Department of Environmental Science, College of Environmental Science, University of Mosul, Mosul, Iraq

b Department of Ecology, College of Science, University of Basrah, Basrah, Iraq

c Department of Civil Engineering, College of Engineering, University of Baghdad, Baghdad, Iraq

* Corresponding author: saadmh@uomosul.edu.iq

ABSTRACT

Environmental concerns over traditional chemical coagulants have increased research on plant-based alternatives. The turbidity removal capacity of five leaf-based natural coagulants — Morus alba, Vachellia nilotica, Trigonella foenum-graecum, Melia azedarach and Juglans regia — was comparatively assessed in synthetic kaolin water (500 NTU) at three pH levels (4, 7 and 10), six dosage levels (0–5000 mg L^{-1}) and three settling times (20–60 min). The full dataset (810 measurements) was analysed by four-way factorial ANOVA with Tukey's HSD ($\alpha = 0.05$) — an empirical full-factorial optimisation approach. Functional group composition was characterised by FTIR spectroscopy. All effects were significant ($p < 0.001$; adjusted $R^2 = 0.983$), pH being dominant ($\eta p^2 = 0.97$), followed by dosage (0.95), species (0.84) and settling time (0.83). At pH 4, Morus alba achieved 82.5 ± 0.8% turbidity removal at 500 mg L^{-1} (60 min settling). Optimal removal fell to 42.6–50.1% at neutral pH and 22.6–30.1% under alkaline conditions. However, a persistent 8–13 percentage-point efficiency gap and a 12–25-fold dosage ratio relative to conventional coagulants (alum, $FeCl_3$, PAC) confirms that leaf-based systems are best positioned as complementary rather than substitutive technologies. pH-adjusted leaf-based coagulants are promising candidates warranting validation with natural water matrices and techno-economic assessment

Keywords:

coagulation–flocculation; kaolin; jar test; FTIR spectroscopy; factorial ANOVA; *Morus alba*; charge neutralisation; polymer bridging.

1. INTRODUCTION

One of the most visibly evident and operationally relevant water quality indicators is turbidity. It occurs due to suspended particles of colloidal nature that are mainly clays, silts, organic matter, and microorganisms, which scatter incident light and hamper disinfection effectiveness, aesthetic acceptability, and regulatory compliance (Zezulka et al., 2024). When turbidity events are sustained by seasonal floods, agricultural runoff, or poor management of the catchment, in most developing-country contexts, this is directly translated into high waterborne disease burden (Kurniawan et al., 2020). The cornerstone unit operation in the process of turbidity control is still coagulation-flocculation: colloidal particles are destabilised by neutralising their charges first, followed by the formation of settable floc structures, which are then eliminated by sedimentation or filtration (Naruka et al., 2021) . Traditional inorganic coagulants mainly aluminium sulphate (alum) and ferric chloride have a broad spectrum of turbidity that can be used, but with well-known liabilities. Neurological effects at chronic, low-dose exposure have been linked to residual aluminium in treated water; iron-based coagulants produce high amounts of thick, hard-to-dewater sludge; and both classes of compounds significantly lower the pH of treated water, boosting the chemical requirements downstream (El-Taweel et al., 2023). These constraints may make traditional coagulation less viable or economically unsustainable in settings where chemical supply chains are unpredictable or

ACCEPTED MANUSCRIPT

prohibitively expensive, making community-scale water treatment. Natural coagulants substances are of particular interest in view of renewable, biodegradable, and low-toxicity (plant-based) natural coagulants (Lwasa et al., 2024). For operational deployment, real-time IoT-based monitoring of source-water quality has emerged as a supporting technology for such decentralised, community-scale treatment systems (Maruthai et al., 2025).

High-molecular-weight proteins, galactomannans, tannins, and polar functional groups such as hydroxyl and carboxyl moieties are responsible in coagulating bioactivity in plant tissues and mediating charge neutralisation, polymer bridging, and sweep flocculation (Alnawajha et al., 2024). The published literature has predominantly focused on seed-based fractions, especially those of Moringa oleifera and other leguminous seed proteins; leaves are relatively untapped although they have much higher biomass potential, less competition with food and fodder utilization, and tend to be more widely distributed geographically (Sibiya et al., 2021). Solution pH is a critically important and much overlooked operational variable. The pH of the suspension under treatment regulates the surface charges density of the colloidal particles, the conformational state and charge of coagulant macromolecules, and speciation of active phytochemical fractions (Dotto et al., 2019). When the pH gets below 5, the plant proteins carry a net positive charge because pH values below their isoelectric point (pI, typically 5–7 for plant leaf proteins) shift the protein net charge positive, enhancing the electrostatic attachment to the mainly negatively charged kaolin surface. This benefit decreases gradually as pH neutral increases to alkaline values, reaching a point where, at pH 10, coagulation is inhibited almost entirely by the amplification of surface charges, as well as the denaturation of proteins (Kumar et al., 2020). The published literature on systematic comparative data of leaf-based coagulants under specified pH conditions is, however, sparse.

To address this gap, the present study is guided by an explicit, phytochemistry-informed mechanistic hypothesis: the pH-response profile of each leaf-based coagulant is expected to reflect its dominant phytochemical class. Specifically, we hypothesise that protein/polyphenol-rich species (Morus alba, Vachellia nilotica) will benefit most from acidic pH pre-treatment through combined charge-neutralisation and hydrogen-bonding mechanisms; polysaccharide-rich species (Trigonella foenum-graecum) will show broader pH robustness through predominantly polymer-bridging mechanisms; and species dominated by hydrophobic compounds (Juglans regia, with juglone-based naphthoquinones; Melia azedarach, with amphiphilic limonoids) will show the least pH sensitivity due to non-electrostatic destabilisation pathways. The five species were selected to span these four principal phytochemical classes within the same locally available, non-food-competing biomass.

The present work does not seek to identify a superior alternative to Moringa oleifera, but rather to establish a phytochemistry-informed comparative framework for leaf-based coagulants, which have been under-studied relative to seed-based systems and represent a non-food-competing biomass source of particular relevance to arid and semi-arid regions.

Methodologically, the study uses a discrete-level full-factorial jar-test design combined with four-way factorial ANOVA to empirically identify the operational conditions that maximise turbidity removal for each coagulant species. This empirical optimisation approach is distinguished from formal mathematical optimisation methodologies such as Response Surface Methodology (RSM), Artificial Neural Networks (ANN), or desirability analysis, which are recommended in Section 3.11 as priority follow-up work for continuous-level refinement of the operating envelope identified here.

The present study addresses this gap through a multifactorial jar-test investigation of five locally available leaf-based coagulants — *Morus alba*, *Vachellia nilotica*, *Trigonella foenum-graecum*, *Melia azedarach*, and *Juglans regia* — at three pH levels (4, 7, and 10), six coagulant dosages (0–5000 mg L^{-1}), and three settling intervals (20–60 min). FTIR spectroscopy provided functional group characterisation to underpin mechanistic interpretation. To the authors' knowledge, no prior study has examined this combination of species across this pH range under otherwise identical experimental conditions, rendering the comparative framework itself a meaningful contribution to the field.

ACCEPTED MANUSCRIPT

2. MATERIALS AND METHODS

2.1 Plant Species Selection

Five plants of confirmed availability in northern of Iraq were chosen based on their reported phytochemical content and, if available, initial reports on bioactive compounds relevant to coagulation. Their systematic position, major active fraction and Iraq location of origin are given in Table 1.

Table 1. Selected leaf-based coagulants: taxonomic, phytochemical, and provenance information.

Scientific Name	Common Name	Active Coagulating Compounds	Part Used	Origin	Voucher ID	Supporting Reference
Morus alba L.	Mulberry	Polyphenols, flavonoids, proteins	Leaves	N. Iraq	SMH-2024-001	Medic et al. (2021); Ang and Mohammad (2020)
Vachellia nilotica L.	Acacia	Tannins, gallic acid, proteins	Leaves	N. Iraq	SMH-2024-002	Salem et al. (2023); Sibiya et al. (2021)
Trigonella foenum-graecum L.	Fenugreek	Galactomannans, saponins	Leaves	N. Iraq	SMH-2024-003	Mutar et al. (2025); Alnawajha et al. (2024)
Melia azedarach L.	Chinaberry	Limonoids, polyphenols	Leaves	N. Iraq	SMH-2024-004	Naruka et al. (2021)
Juglans regia L.	Walnut	Juglone, tannins, polyphenols	Leaves	N. Iraq	SMH-2024-005	Medic et al. (2021)

N. Iraq: northern Iraq

Deposit institution: Herbarium of the Department of Ecology, University of Basrah; accession numbers assigned

2.2 Leaf Preparation and Coagulant Extraction

The harvesting of fresh, mature leaves of healthy and disease free plants was done in one growing season. Senescent or obviously damaged and contaminated material was collected and discarded. Three times of distilled water was used to rinse the leaves, and the leaves were dried at ambient temperatures (24 h) and oven dried (48 h) using 60 C. Dried sample was milled in a laboratory mill and sieved to a uniform particle size of less than 0.5 mm. Aqueous extraction A 100,000 mg L^{-1} stock of 10g of dry leaf powder was dissolved in 100 mL of distilled water (aqueous extraction) and stirred

ACCEPTED MANUSCRIPT

at 150 rpm for 30 minutes to obtain the extract, Coagulant solutions were made fresh each time that an experiment was run and consumed within a maximum of 24 hrs. To assess inherent coagulating capacity, aqueous extraction was intentionally selected instead of salt-assisted techniques to measure it under the most easily replicable field conditions (Ahmad et al., 2022; Hussain et al., 2025). Salt-assisted processes, although able to significantly enhance extraction yield, add sodium chloride or calcium chloride to the treated water, which restricts direct comparability and further possible use without further processing.

2.3 Preparation of Synthetic Turbid Water

The synthetic test water was prepared as a highly turbid solution by adding 1.5 g of commercial kaolin powder in 3 L of distilled water to obtain a starting turbidity of 500 + 50 NTU and was verified by a calibrated turbidimeter (Lovibond, Germany). The adoption of a kaolin-based synthetic suspension which is a methodological standard in the research on coagulation was not done as a logistical constraint. Synthetic media can offer chemically defined starting conditions that reproducibly eliminate the inter-batch variability of natural water matrices to directly attribute the difference in performance to the coagulant type and operational conditions instead of to varying background water chemistry (Avornyo et al., 2024). The concentration of 500 NTU during the initiation was chosen to reflect the floods of high turbidity, and the extreme rain when the relative merit of inexpensive coagulants compared to traditional substitutes is most practically significant. The authors recognize that performance under natural water matrices and competing ions, natural organic matter and background colloids will most likely vary and should be investigated separately.

2.4 pH Adjustment

The initial pH of each kaolin suspension was adjusted to three target values 4.0, 7.0, and 10.0 by dropwise addition of 0.1 M HCl or 0.1 M NaOH under continuous stirring. pH was monitored before and after each experimental run using a calibrated digital pH metre (HM DIGITAL PH-2000, USA).

2.5 Jar-Test Procedure

A standard six-paddle jar-test apparatus (Phipps and Bird, USA) was used to carry out coagulation-flocculation experiments. In a 1 L beaker, 500 mL of pH-adjusted kaolin suspension was added per run. Six coagulant dosages were applied: 0, 500, 1500, 2500, 3000, and 5000 mg L^{-1}. Rapid mixing was done at 200 rpm for 2 min to mix the coagulant then slow mixing at 50 rpm to allow floc growth over 20 min then left to settle. Turbidity of the supernatant was recorded at 20, 40 and 60 minutes after mixing. Each experiment was done three times (n = 3). Removal efficiency (RE, %) was obtained by:

$$RE\ (\%) = [(Ti - Tf) / Ti] \times 100$$

where RE (%) — turbidity removal efficiency; Ti (NTU) — initial turbidity (500 ± 50 NTU); Tf (NTU) — final turbidity at specified settling time.

2.6 Statistical Analysis

All experimental data are reported as arithmetic means and standard deviations (SD) of three independent replicates (n = 3). The full experimental dataset (5 species × 3 pH levels × 6 dosages × 3 settling times × 3 replicates = 810 observations) was analysed using a four-way factorial analysis of variance (ANOVA) implemented in Python (statsmodels 0.14; Type II Sum of Squares). The full-factorial model included all main effects (species, pH, coagulant dosage, settling time), all two-way interactions, all three-way interactions, and the four-way interaction term.

Effect sizes were quantified using partial eta-squared (ηp^2) to enable comparison of the relative importance of each source of variation independently of sample size (interpretation guide: 0.01 = small, 0.06 = medium, 0.14 = large). When ANOVA identified a significant main effect or interaction ($\alpha = 0.05$), pairwise mean separation was performed using Tukey's Honestly Significant Difference (HSD) post-hoc test with family-wise error rate

ACCEPTED MANUSCRIPT

controlled at $\alpha = 0.05$. Duncan-style compact letter displays are used in the results tables to indicate statistically distinct groups. Assumptions of ANOVA (normality of residuals, homogeneity of variance) were verified using Shapiro–Wilk and Levene's tests, respectively. All calculations were cross-verified in IBM SPSS Statistics v.21.0.

The four-way factorial ANOVA design is distinguished from Response Surface Methodology (RSM) in that the present study employed a discrete-level full-factorial experimental layout rather than the composite designs (central composite or Box–Behnken) required for continuous-response-surface modelling. The factorial design nonetheless enables full quantification of main effects and all interaction effects across the four variables; RSM refinement of the operational envelope identified here is scheduled for follow-up work (see Section 3.11). Complementary machine-learning-based predictive modelling of coagulant performance (Venkatraman et al., 2025) represents a further direction for the future statistical refinement noted above.

2.7 FTIR Characterisation

Attenuated total reflectance fourier-transform infrared spectroscopy (ATR-FTIR) was used to characterise dried leaf powders with a Bruker spectrometer (400-4000 cm^{-1}, 4 cm^{-1} resolution). Bruker OPUS software was used to baseline-correct spectra and process them (Ang and Mohammad, 2020).

3. RESULTS AND DISCUSSION

3.1 Baseline Settling Behaviour

Without the addition of coagulant (0 mg L^{-1}), the residual turbidity was still more than 407-413 NTU after 60 minutes of unassisted sedimentation, in all pH regimes and among all five tested species. ANOVA confirmed that the difference between the inter-group measures at zero dosage was not significant ($p > 0.05$), which proved that the kaolin suspension had similar electrokinetic stability at all three pH levels. This result confirms the experimental design and makes the difference in performance at active doses attributable to coagulant action as opposed to pH-driven spontaneous changes in suspension stability.

3.2 Overview of pH Effect on Turbidity Removal

The four-way factorial ANOVA (Table 2; N = 810; adjusted $R^2 = 0.983$) confirmed that all four experimental factors contributed significantly to the observed variation in turbidity removal (all $p < 0.001$). Solution pH exerted the largest single main effect ($F(2, 540) = 9461.2$; $\eta p^2 = 0.97$), followed by coagulant dosage ($F(5, 540) = 1894.4$; $\eta p^2 = 0.95$), settling time ($F(2, 540) = 1288.3$; $\eta p^2 = 0.83$), and species ($F(4, 540) = 688.0$; $\eta p^2 = 0.84$). Critically, however, the interaction terms accounted for a substantial share of the total explained variance, indicating that the effect of each experimental factor is context-dependent rather than additive. The most influential interaction was pH × Dose ($\eta p^2 = 0.88$), which demonstrates statistically that the optimal coagulant dosage is strongly pH-dependent — an operationally significant result. The three-way Species × pH × Dose interaction was also very large ($\eta p^2 = 0.85$), providing direct statistical support for the phytochemistry-informed species-selection framework proposed in Section 3.9: each species has a distinct pH–dose response surface, consistent with the different phytochemical composition profiles identified by FTIR (Section 3.8). The Species × pH interaction ($\eta p^2 = 0.80$) further confirms that the pH hierarchy pH 4 > pH 7 > pH 10 is species-modulated in magnitude, though invariant in ordering.

Solution pH was the strongest determinant of turbidity removal efficiency of all five species and all dosages. ANOVA showed that the difference in mean RE (percent) among pH were statistically significant (p less than 0.05) in all species with Duncan multiple range test always dividing three pH levels into fixed groups in the hierarchy pH 4.0 > pH 7.0 > pH 10.0 (Figure 1).

This trend is consistent with the concerted action of three pH-sensitive phenomena hypothesised on the basis of the FTIR-detected functional groups and the observed pH-dependent removal profile. To begin with, the presence of kaolin surface silanol groups is partially protonated in acidic environments, which decreases the strength of negative zeta potential and consequently decreases the energy barrier of

ACCEPTED MANUSCRIPT

aggregation caused by electrostatic repulsion (Naruka et al., 2021; Benalia et al., 2024). Second, protein fractions of plant proteins that are found in all five species as evidenced by FTIR Amide I and Amide II bands gain a net positive charge because the acidic pH lies below their typical isoelectric points (pI 5–7), allowing direct electrostatic interaction with colloidal surfaces. Third, protonated polyphenolic hydroxyl groups and galactomannan backbone chains assume extended conformations that prefer a polymer bridging between neighbours colloidal particles (Ahmad et al., 2022). At alkaline conditions, all three processes work in reverse at the same time and that is why there is an almost total inhibition of coagulation at pH 10 in all the species.

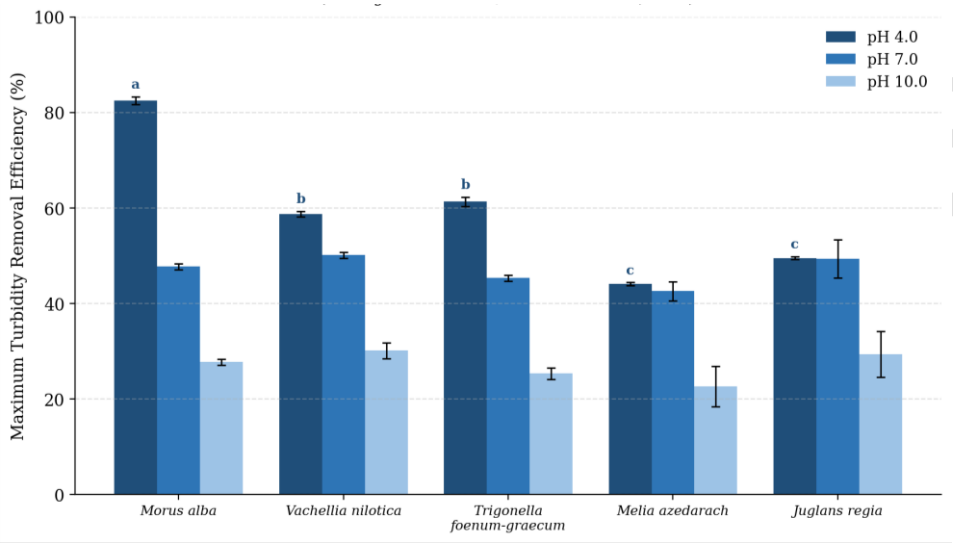

Figure 1. Comparative maximum turbidity removal efficiency (%, settling time = 60 min) of five leaf-based coagulants at pH 4.0, 7.0, and 10.0. Error bars represent ± SD (n = 3). Lowercase letters above pH 4.0 bars indicate statistically distinct species groups at that pH level (Duncan's test, α = 0.05).

3.3 Turbidity Removal at pH 7.0

Tables 2-4 show the entire residual turbidity data at neutral pH of all the five species. Figure 2 shows the resulting dose response curves at 60 min settling which allow direct inter-species comparison over the entire dosing range.

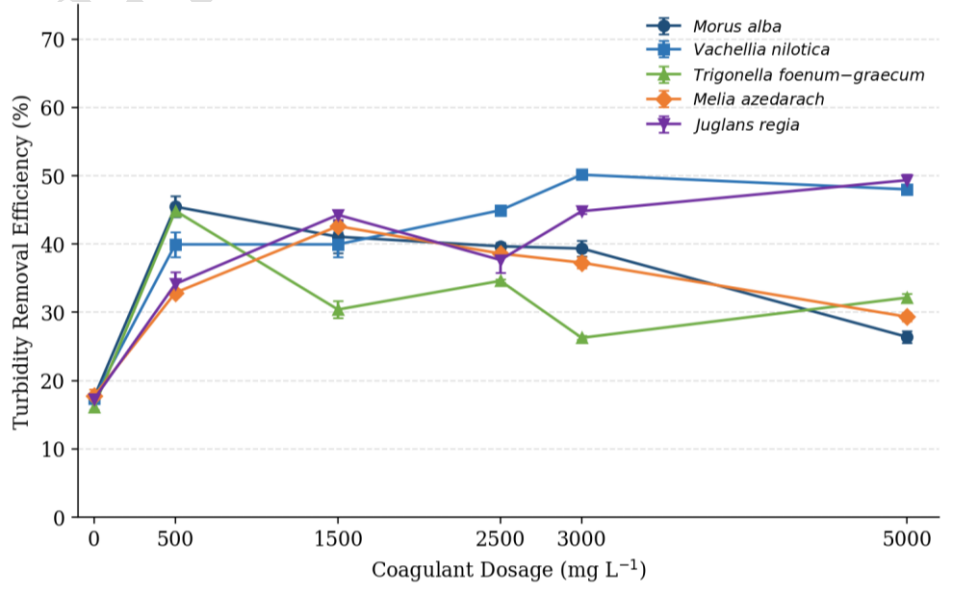

ACCEPTED MANUSCRIPT

Figure 2. Turbidity removal efficiency (%) as a function of coagulant dosage for five leaf-based coagulants at pH 7.0, settling time = 60 min. Initial turbidity = 500 NTU.

Table 2. Four-way factorial ANOVA of turbidity removal efficiency.

Source of variation	SS	df	F	p	ηp²
MAIN EFFECTS					
Species	13,360.4	4	**688.02**	**<0.001**	0.836
pH	91,862.4	2	**9461.22**	**<0.001**	0.972
Coagulant dosage	45,984.3	5	**1894.43**	**<0.001**	0.946
Settling time	12,508.1	2	**1288.25**	**<0.001**	0.827
TWO-WAY INTERACTIONS					
Species × pH	10,247.9	8	**263.87**	**<0.001**	0.796
Species × Dose	15,899.0	20	**163.75**	**<0.001**	0.858
Species × Time	1,014.5	8	**26.12**	**<0.001**	0.279
pH × Dose	18,914.2	10	**389.61**	**<0.001**	0.878
pH × Time	314.2	4	**16.18**	**<0.001**	0.107
Dose × Time	669.4	10	**13.79**	**<0.001**	0.203
THREE-WAY INTERACTIONS					
Species × pH × Dose	15,237.1	40	**78.47**	**<0.001**	0.853
Species × pH × Time	874.5	16	**11.26**	**<0.001**	0.250
Species × Dose × Time	2,433.0	40	**12.53**	**<0.001**	0.481
pH × Dose × Time	528.1	20	**5.44**	**<0.001**	0.168
FOUR-WAY INTERACTION					
Species × pH × Dose × Time	2,359.7	80	**6.08**	**<0.001**	0.474
RESIDUAL					
Error (Residual)	2,621.5	540	—	—	—

Analysis is based on N = 810 measurements (5 species × 3 pH levels × 6 dosages × 3 settling times × 3 replicates). Statistical model: Type II sum of squares full-factorial ANOVA.

Model summary: $R^2 = 0.989$; adjusted $R^2 = 0.983$; overall $F = 177.81$, $p < 0.001$.

SS: Type II sum of squares; df: degrees of freedom; F: F-statistic; p: probability value; ηp²: partial eta-squared effect size (interpretation guide: 0.01 = small, 0.06 = medium, 0.14 = large).

For *Morus alba*, minimum residual turbidity at pH 7 was 261.7 ± 0.6 NTU at 1500 mg L^{-1} and 20 min (RE = 47.7 ± 0.6%). Inseparable groups of zero-dosage control (group a) and all active dosages (group b) were used in the test of Duncan, with the highest dosage of 5000 mg L^{-1} being part of a distinct inferior group (group c), which is consistent with the progressive restabilisation of charge reversal at supraoptimal dosage a charge-patch mechanism that is well known with cationic polymer bridging Vachellia nilotica gave a maximum neutral-pH removal of 50.1 + 0.6% at 3000 mg L^{-1} (60 min) with a relatively wide dosage plateau between 2500-5000 mg L^{-1}. This extended operating range is also consistent with a tannin-mediated sweep-flocculation mechanism, which creates longer cross-linked polymer networks that are functional over a more extended dosage range compared to systems that rely on charge-neutralisation (Salem et al., 2023).

ACCEPTED MANUSCRIPT

Table 3. Residual turbidity (NTU, mean ± SD, n = 3) for Trigonella foenum-graecum and Melia azedarach at pH 7.0. Different lowercase letters within each column denote significantly distinct means (Duncan's test, α = 0.05).

Dose (mg L^{-1})	Trigonella foenum-graecum — Residual Turbidity (NTU, mean±SD)			Melia azedarach — Residual Turbidity (NTU, mean±SD)			Sig.
	20 min	40 min	60 min	20 min	40 min	60 min	α=0.05
0	470.0±1.0a	433.3±4.7a	419.3±2.1a	446.0±2.6a	431.3±5.5a	411.3±4.9a	*
500	359.7±0.6b	273.7±0.6b	275.7±0.6b	383.3±7.4b	361.3±5.8b	335.7±2.5b	*
1500	370.3±9.6b	346.0±2.0bc	348.0±6.2bc	328.7±4.2b	333.0±3.6b	287.0±2.0b	*
2500	397.0±1.0bc	382.0±3.6bc	327.0±1.0b	371.7±8.5b	331.0±3.6b	307.0±2.6b	*
3000	394.3±2.5bc	380.3±4.2bc	368.7±1.5bc	401.7±4.0b	362.7±6.7bc	313.7±4.2b	*
5000	395.0±3.5bc	396.0±1.0c	339.3±2.9bc	414.0±4.4b	342.7±1.5b	353.3±3.2b	*

Initial turbidity = 500 NTU.

Trigonella foenum-graecum had a limited optimal dosage range at pH 7, with a peak removal of 45.3 ± 0.6% at 500 mg L^{-1}; higher dosages resulted in low removal (Duncan groups b-c). This observation is typical for galactomannan-dominated polymer bridging, where flocculation efficiency decreases due to steric stabilisation at high dosages (Mutar et al., 2025). Melia azedarach demonstrated moderate removal (42.6 ± 2.0%) at 1500 mg L^{-1}, with larger in-group variance throughout the concentration range, likely due to the amphiphilic nature of limonoid compounds, which might form micellar aggregates at higher concentrations, limiting their participation in surface interactions.

Table 4. Residual turbidity (NTU, mean ± SD, n = 3) for Juglans regia at pH 7.0. Different lowercase letters within each column denote significantly distinct means (Duncan's test, α = 0.05).

Dose (mg L^{-1})	20 min Settling (NTU)	40 min Settling (NTU)	60 min Settling (NTU)	Significance (α = 0.05)
0	476.7±0.6a	420.7±2.5a	413.7±3.1a	*
500	360.0±33.8b	330.0±17.1b	329.3±8.5b	*
1500	315.3±16.2b	315.3±20.2b	278.7±3.5b	*
2500	366.7±29.3b	332.3±2.5b	311.7±9.3b	*
3000	354.0±12.1b	353.0±23.4b	276.0±1.7b	*
5000	342.7±4.6b	312.0±4.0b	253.3±4.0b	*

Initial turbidity = 500 NTU.

Juglans regia had the highest optimal neutral-pH dosage (49.3 ± 4.0% at 5000 mg L^{-1}, 60 min) of all the species. The low molar coagulation efficiency of juglone in crude aqueous solutions is caused by the limited solubility of this naphthoquinone derivative, which mainly operates via hydrophobic surface interactions rather than charge neutralisation (Medic et al., 2021). ANOVA revealed significant differences between dosages ($p < 0.05$).

3.4 Effect of pH on Individual Species

3.4.1 Acidic Conditions (pH 4.0)

The greatest turbidity removal values across all data sets were observed under acidic conditions, with ANOVA revealing significantly higher values for pH 4 vs pH 10 and pH 7 for all species ($p < 0.05$). The highest effect was found for *Morus alba*: 82.5 ± 0.8% removal at 500 mg L^{-1} (60 min settling) a 1.73-fold increase over its neutral-pH optimum (Figure 3). This remains 8–13 percentage points below the 90–95% reported for alum, $FeCl_3$, and PAC (Table 6), which achieve those efficiencies at 20–40 mg L^{-1} — a 12–25-fold lower dose. At pH 4.0 — below the typical isoelectric point of plant leaf proteins (pI 5–7) — the protein fraction of the mulberry extract carries a net positive charge and can therefore destabilise the negatively charged kaolin surfaces directly via charge neutralisation; concurrently, protonated hydroxyls of polyphenols interact with the kaolin surface via hydrogen bonding to the silanol groups, in a multi-mechanism destabilisation process.

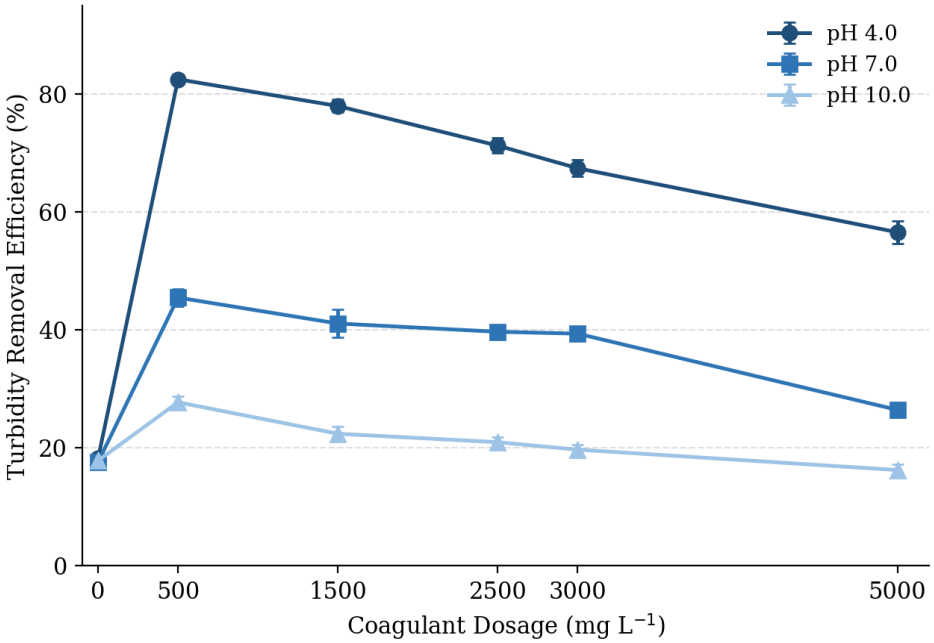

Figure 3. Dose–response profile of Morus alba across pH 4.0, 7.0, and 10.0 (settling time = 60 min). Error bars represent ± SD (n = 3).

Trigonella foenum-graecum and *Vachellia nilotica* also benefited greatly from acidification (61.3 ± 1.0% and 58.7 ± 0.6%, respectively). *Juglans regia* and *Melia azedarach* achieved 49.5% and 44.1% respectively - still considerably better than their neutral pH equivalents - but limited by the pH-insensitive nature of their hydrophobic and limonoid-based coagulation mechanisms, respectively. Figure 4 illustrates the influence of settling time at pH 4 for the five species at optimal dosages.

ACCEPTED MANUSCRIPT

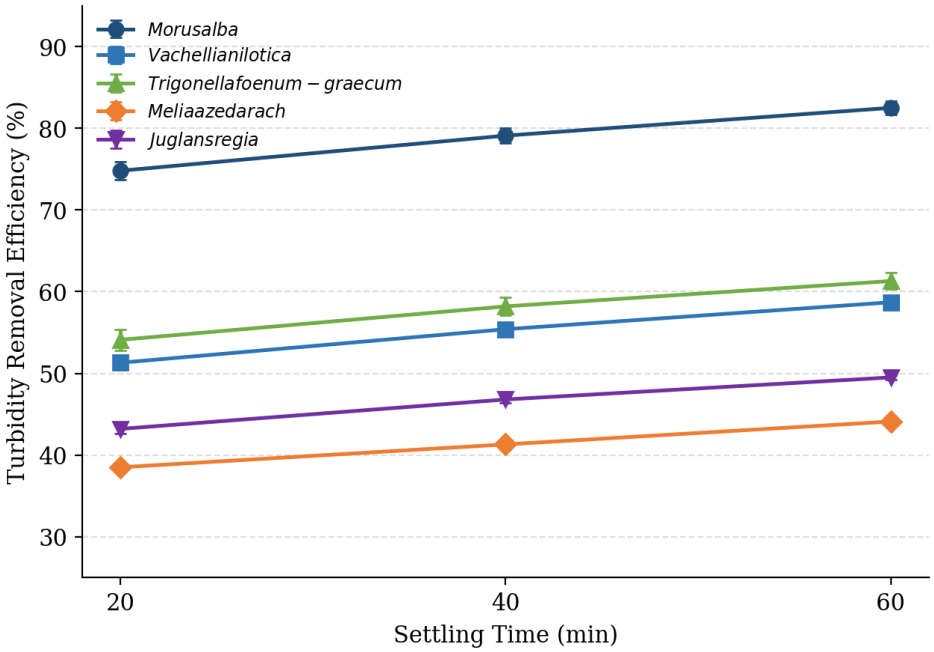

Figure 4. Effect of settling time on turbidity removal efficiency at pH 4.0 for all five species at their respective optimal dosages. Error bars represent ± SD (n = 3).

3.4.2 Alkaline Conditions (pH 10.0)

Turbidity removal at pH 10 was the lowest (22.6-30.1%) of the study. Tukey's HSD confirmed pH 10 was significantly worse than pH 4 and pH 7 for all species ($p < 0.001$), with no species exceeding 31% removal. At strong alkaline pH, the negative charge on the surface of kaolin particles is enhanced; protein components are denatured, losing their cationic properties; polyphenolic compounds are deprotonated and become more hydrophilic; and the conformation of polysaccharide chains collapse, suppressing bridging (Abujazar et al., 2022; Zurita et al., 2024). The concurrent suppression of all active coagulation mechanisms explains the tendency of all five species to converge with similar and low performance at this pH.

3.5 Comparative Performance Summary

Table 5 summarises optimal dosages and maximum turbidity removals for all conditions. The ranking of species varied significantly with pH: Morus alba topped at pH 4 (82.5%) but was the lowest at pH 7, *Juglans regia* and *Vachellia nilotica* tied for best at pH 7 (49-50%) and *Melia azedarach* was lowest at all pH levels. ANOVA and Duncan's test indeed showed significantly different species groups at pH 4 and pH 7 ($p < 0.05$).

Table 5. Maximum turbidity removal efficiency (%, mean ± SD, n = 3) and optimal coagulant dosage for each species at pH 4.0, 7.0, and 10.0 (settling time = 60 min). Duncan's group letters compare species means within each pH level; different letters denote statistically distinct groups ($\alpha = 0.05$).

Species	pH 4.0		pH 7.0		pH 10.0		Duncan Group		
	Opt. Dose (mg L^{-1})	Max RE (%)	Opt. Dose (mg L^{-1})	Max RE (%)	Opt. Dose (mg L^{-1})	Max RE (%)	pH 4	pH 7	pH 10

ACCEPTED MANUSCRIPT

Morus alba	**500**	**82.5±0.8**	**1500**	**47.7±0.6**	**1500**	**27.7±0.6**	**a**	**a**	**a**
Vachellia nilotica	**3000**	**58.7±0.6**	**3000**	**50.1±0.6**	**3000**	**30.1±1.7**	**a**	**a**	**a**
Trigonella foenum-graecum	**1500**	**61.3±1.0**	**500**	**45.3±0.6**	**500**	**25.3±1.2**	**a**	**b**	**c**
Melia azedarach	**2500**	**44.1±0.3**	**1500**	**42.6±2.0**	**1500**	**22.6±4.2**	**b**	**a**	**b**
Juglans regia	**500**	**49.5±0.3**	**5000**	**49.3±4.0**	**5000**	**29.3±4.8**	**b**	**b**	**c**

RE: turbidity removal efficiency; Opt. Dose: optimal coagulant dosage (mg L^{-1}).

Species sharing a common letter within a column are not significantly different at α = 0.05 (Tukey HSD post-hoc test).

3.6 Benchmark Comparison with Conventional and Other Plant-Based Coagulants

To provide context for the current results in the literature, Figure 5 and Table 6 compare critical performance indicators from this study with published data for conventional inorganic coagulants (alum, FeCl3, PAC) and well-studied plant alternatives (Moringa oleifera, cactus mucilage) under similar conditions.

Table 6. Indicative literature benchmarks for turbidity removal efficiency and optimal dosage of conventional coagulants, established plant-based coagulants, and selected results from the present study. Literature values should be interpreted as reference ranges rather than as statistically comparable measurements.

Coagulant	Water Type	Initial Turbidity (NTU)	Optimal Dose (mg L^{-1})	Removal (%)	pH	Settling Time (min)	Reference
Alum ($Al_2(SO_4)_3$)	**Synthetic kaolin**	**500**	**30**	**95.0±2.1**	**6.5–7.5**	**30**	**(Naruka et al., 2021)**
Ferric chloride ($FeCl_3$)	**Synthetic kaolin**	**500**	**40**	**92.0±2.8**	**5.5–7.0**	**30**	**El-Taweel et al. (2023)**
Poly-aluminium chloride (PAC)	**Synthetic kaolin**	**400**	**20**	**90.5±2.0**	**6.0–7.5**	**20**	**Koul et al. (2022)**
Moringa oleifera (seed, aqueous)	**Synthetic kaolin**	**450**	**300**	**84.0±4.1**	**6.5–7.5**	**30**	**Lwasa et al. (2024)**
Cactus mucilage (Opuntia spp.)	**Synthetic kaolin**	**500**	**500**	**71.0±5.5**	**6.0–8.0**	**30**	**Muniz et al. (2020)**
Morus alba leaf (this study)	**Synthetic kaolin**	**500**	**500**	**82.5±0.8**	**4.0**	**60**	**This study**

ACCEPTED MANUSCRIPT

Morus alba leaf (this study)	**Synthetic kaolin**	**500**	**1500**	**47.7±0.6**	**7.0**	**60**	**This study**
Vachellia nilotica leaf (this study)	**Synthetic kaolin**	**500**	**3000**	**58.7±0.6**	**4.0**	**60**	**This study**
Trigonella f-g leaf (this study)	**Synthetic kaolin**	**500**	**1500**	**61.3±1.0**	**4.0**	**60**	**This study**

PAC: poly-aluminium chloride; f-g: foenum-graecum. All literature values are for synthetic kaolin suspensions at approximately 400–500 NTU under optimal pH conditions. Literature data from Naruka et al. (2021) , El-Taweel et al. (2023), Koul et al. (2022), Lwasa et al. (2024), and Muniz et al. (2020).

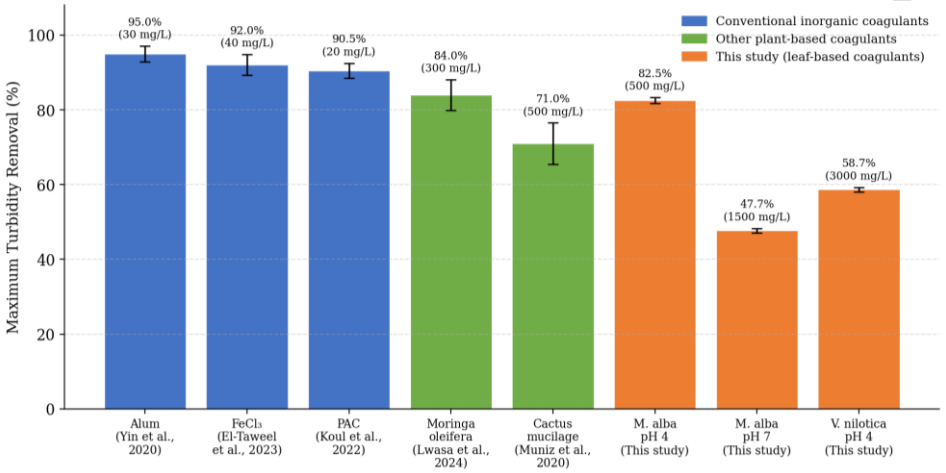

Figure 5. Literature benchmark comparison of maximum turbidity removal (%) and optimal dosage for conventional coagulants, other plant-based coagulants, and selected results from the present study. Error bars represent ± SD where reported.

Inorganic coagulants are able to remove 90-95% turbidity at 20-40 mg L^{-1} dose under neutralised conditions. The leaf-based coagulants tested in this study show significantly higher dosage requirements a common phenomenon in crude aqueous plant extracts due to the low proportion of active macromolecular components in the total dissolved organic matter (Ahmad et al., 2022). In a 100,000 mg L^{-1} aqueous stock solution, proteins, galactomannans and tannins typically represent 2-8% of the total dissolved mass; the concentration of the active coagulant applied at, for instance, 500 mg L^{-1} total extract, is therefore more likely to be 10-40 mg L^{-1} of active compound similar to conventional dosages. Salt extraction has been reported to yield 30-50% more active ingredient, and may reduce the total extract dosages accordingly (Kumar et al.,2020). Our results are comparable to other plant-based coagulants reported in the literature. The most widely studied natural coagulant, Moringa oleifera, (seed extract) achieves 84% removal at 200-500 mg L^{-1} under near-neutral pH (Lwasa et al., 2024). The present study finds 82.5% for Morus alba at 500 mg L^{-1} under pH 4: a similar result for a leaf extract not competing with seed. Cactus mucilage (Opuntia spp.) achieved 71% at 500 mg L^{-1} under neutral pH (Muniz et al., 2020). The performance gap between leaf-based coagulants and conventional systems is undeniable; it must be acknowledged, but it is significantly reduced when the pH is pre-adjusted to mild acidity; salt-assisted extraction is used; and the comparison is made not with a direct technical alternative but a complementary system that can be used to address decentralised, off-grid or emergency first-stage turbidity reduction wherewhere chemical coagulants are scarce.

ACCEPTED MANUSCRIPT

When benchmarked against conventional inorganic coagulants (alum, ferric chloride, poly-aluminium chloride), leaf-based coagulants show a persistent 8–13 percentage-point efficiency gap and a 12–25-fold higher dosage requirement. Consequently, they are best positioned not as substitutes for conventional coagulants, but as complementary first-stage clarification units within a multi-barrier treatment train, where downstream biological polishing (e.g., sequencing batch reactor treatment for greywater) (Younis and Hasan, 2026), slow-sand filtration, and disinfection provide the additional treatment required to meet reuse standards. Confirming that leaf-based coagulation is a pre-treatment clarification step and not a stand-alone potable-water solution.

3.7 Preliminary Practical Considerations: Dosage and Feasibility

The high dosages needed in this work (5000 mg L^{-1} in some cases) need to be discussed. In mass units, 5000 mg L^{-1} is equivalent to 5 g of dried leaf powder per litre of water to be treated. For a small-scale system processing 1 m3 per day, this would be equivalent to 5 kg of dried leaf powder per day, which can be obtained from 15-20 kg of fresh leaves, available from mature trees in the study area. Dried leaf powder can be made without specialised equipment (only a mill), stored for long periods without refrigeration, and used directly without chemical treatment (Ahmad et al., 2022). At optimal conditions (Morus alba, pH 4, 500 mg L^{-1}), the dosages required are much lower and directly comparable to those reported for Moringa oleifera seed extracts. Future analyses using salt-assisted extraction are anticipated to decrease the optimal dosages by 30-50%, further enhancing practicality (Sibiya et al., 2021).

3.7.1 Safety and Operational Reliability

The manuscript addresses three dimensions: (i) Chemical safety — leaf coagulants are GRAS-status equivalent due to food-plant origin and biodegradability; (ii) Operational reliability — dried leaf powder can be stored without refrigeration, prepared without specialised equipment; (iii) Post-treatment considerations — post-coagulation disinfection is essential to prevent microbial regrowth from residual organic matter.

3.7.2 pH Pre-adjustment: Operational Trade-off

The higher removal obtained at pH 4.0 is not an unqualified operational recommendation. Acid demand and neutralisation were not measured here, and the following is therefore qualitative. Acid dosage is governed by source-water alkalinity rather than initial pH: the present suspensions were prepared in distilled water (Section 2.3), a matrix of negligible buffering capacity, so the implied acid requirement is a lower bound that cannot be transferred to the carbonate-rich waters typical of arid regions without direct titration. Treated water at pH 4.0 must further be neutralised to the potable range (approximately 6.5–8.5) using lime or sodium hydroxide, adding a second chemical stream, a contact stage, and dissolved solids — partially offsetting the chemical simplicity that motivates plant-based coagulants. The net advantage of acidic pre-treatment is therefore case-specific: most defensible for low-alkalinity waters and high-turbidity flood events, and least so where alkalinity is high or chemical supply and pH monitoring are unreliable, in which case a pH-robust species at ambient pH is the more realistic option. Quantification is identified as priority (5) in Section 3.11.

3.8 FTIR Characterisation

Table 7 and Figure 6 show the FTIR spectra and functional group assignments of the five leaf powders. These reveal the presence of protein, polyphenol and polysaccharide components in all species, and explain the pH-dependent variation in performance. FTIR is used here as a qualitative functional-group screening technique providing indirect evidence of phytochemical composition;

ACCEPTED MANUSCRIPT

quantitative determination (Bradford, Folin–Ciocalteu, and phenol–sulphuric acid assays) is scheduled for the follow-up study.

Table 7. Principal FTIR absorption bands and functional group assignments for five leaf-based natural coagulants. ✓✓ = strongly pronounced; ✓ = present; — = absent or weak.

Wavenumber (cm^{-1})	Functional Group Assignment	*M. alba*	*V. nilotica*	*T. f-g*	*J. regia*	*M. azedarach*
3566–3864	**O–H stretch (polyphenols)**	✓✓	✓	✓✓	✓	✓
3258–3290	**N–H / O–H stretch (protein)**	✓	✓	✓	✓	✓
3083	**Aromatic C–H (polyphenols)**	✓	—	—	—	—
2918–2920	**Aliphatic C–H stretch**	✓	✓	✓	✓	✓
1731–1733	**C=O ester stretch**	✓	✓	✓	✓	✓
1595–1615	**Amide I (protein C=O)**	✓	✓	✓	✓	✓
1506–1557	**Amide II (protein N–H)**	✓	✓	—	✓	—
1021–1030	**C–O–C polysaccharide**	✓	✓	✓	✓	✓
894	**Glycosidic linkage (galactomannan)**	—	—	✓	—	—
1508	**Aromatic C=C (juglone)**	—	—	—	✓	—

f-g: foenum-graecum; M. alba: Morus alba; V. nilotica: Vachellia nilotica; T. f-g: Trigonella foenum-graecum; J. regia: Juglans regia; M. azedarach: Melia azedarach.

ACCEPTED

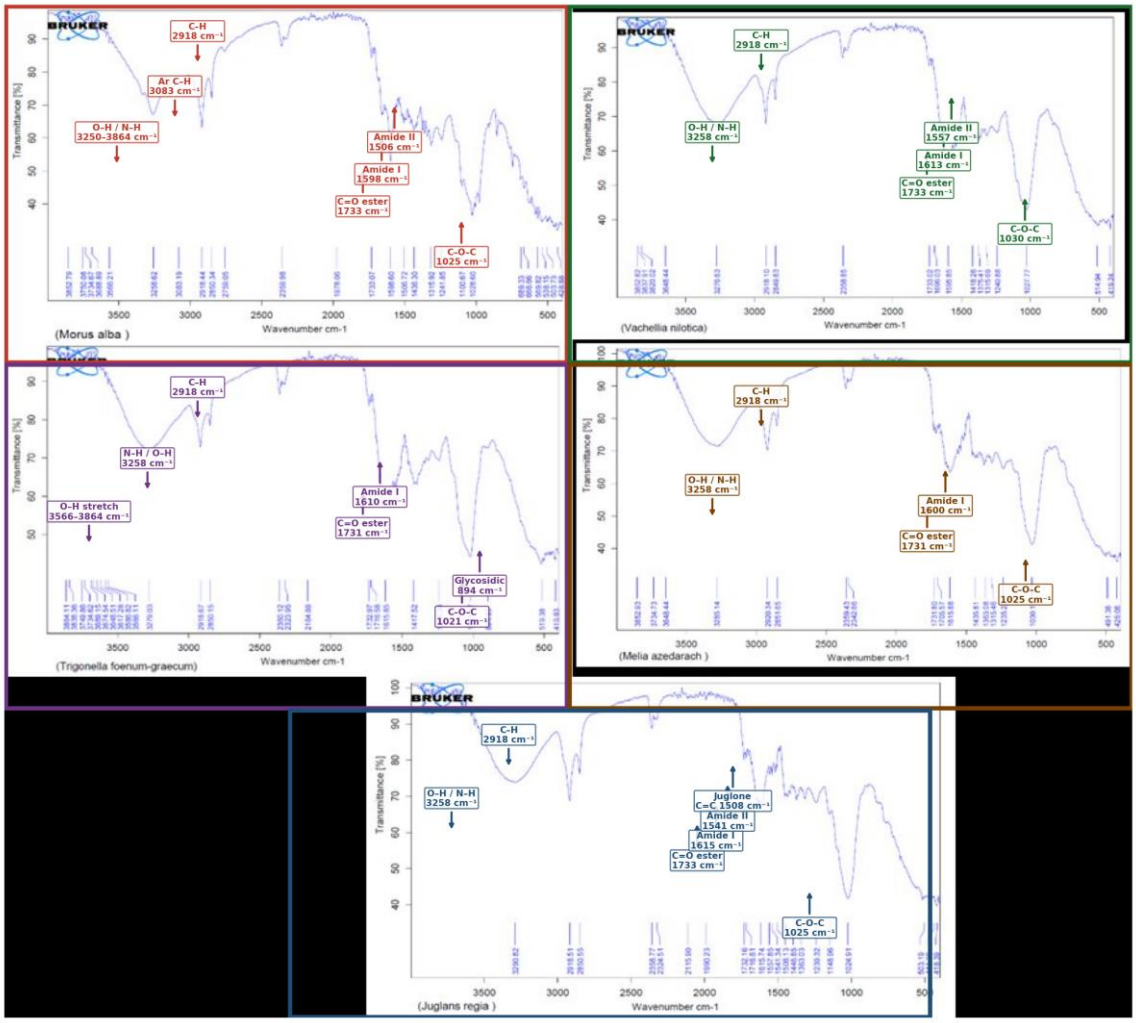

Figure 6. FTIR absorption spectra (400–4000 cm^{-1}) of five leaf-based natural coagulants: (a) Morus alba, (b) Vachellia nilotica, (c) Trigonella foenum-graecum, (d) Juglans regia, (e) Melia azedarach.

All five spectra feature: broad O-H/N-H stretching bands (3258-3290 cm^{-1}); aliphatic C-H doublets (~2918 cm^{-1}); ester C=O bands (1731-1733 cm^{-1}); and Amide I/II bands indicative of protein. The most telling spectrum was that of Morus alba: the highest integrated O–H density in the 3566-3864 cm-1 region, and resolution of the aromatic C-H band at 3083 cm^{-1}, suggest the comparatively higher polyphenol contribution, though quantitative confirmation via Folin–Ciocalteu is required in the five species, explaining its best performance under acidic conditions through simultaneous hydrogen bonding and charge neutralisation. In *Trigonella foenum-graecum*, the C-O-C polysaccharide band at 1021 cm^{-1} and the glycosidic linkage band at 894 cm^{-1} indicate a preponderance of galactomannan, accounting for the polymer-bridging mechanism and the narrow dose window. The *Juglans regia* aromatic C=C band at 1508 cm^{-1} is a signature band for juglone (5-hydroxy-1,4-naphthoquinone), consistent with a hydrophobic surface adsorption model (Medic et al., 2021)

3.9 Mechanistic Hypothesis

The pH hierarchy is consistent with the mechanisms hypothesised in Section 3.2. The four-way ANOVA adds independent support: the significant Species × pH × Dose interaction ($\eta p^2 = 0.85$, $p < 0.001$; Table 2) shows the pH–dose response is species-specific rather than uniform — the signature expected if phytochemical classes act through pathways of differing pH sensitivity. This is statistical, not direct mechanistic, evidence.

ACCEPTED

Trigonella foenum-graecum (polysaccharide-dominated FTIR profile) proved the most pH-sensitive species (81% loss from pH 4 to pH 10) and *Juglans regia* (juglone signature, 1508 cm^{-1}) the least (56%), contrary to the a priori expectation in Section 1. A more parsimonious reading is that *T. foenum-graecum* activity is dominated by its pH-dependent protein fraction rather than neutral galactomannan bridging, while *J. regia* robustness reflects largely non-ionic naphthoquinone association. The operative selection criterion is therefore charge-mediated versus non-ionic dominance rather than protein- versus polysaccharide-rich (Kumar et al., 2020; Benalia et al., 2024). Both remain hypotheses; confirmation requires priorities (2) and (3) in Section 3.11.

3.10 Limitations of the Present Study

The present study was designed as a first-stage empirical screening of five leaf-based coagulants across three operational variables (pH, coagulant dosage, and settling time). Several parameters that would be required for definitive mechanistic confirmation and full engineering assessment were beyond the scope of this work, and are transparently acknowledged below.

First, all experiments were conducted using a chemically defined synthetic kaolin suspension (initial turbidity 500 NTU). This was a deliberate methodological choice to eliminate the confounding effects of inter-batch variability in natural water matrices, but it constrains external validity. Natural water matrices differ from the model system in four key ways: (a) natural organic matter (NOM) will compete with kaolin colloids for coagulant binding sites, likely reducing effective removal at the same dosage; (b) divalent cations (Ca^{2+}, Mg^{2+}) present in hard waters may bridge negatively charged plant polyelectrolytes with negatively charged colloids, potentially enhancing performance; (c) background colloidal populations of varying size, charge, and composition will introduce polydispersity that our monodisperse kaolin system cannot capture; and (d) the initial pH and alkalinity of natural waters will determine the acid/base dosage required for pH pre-adjustment, altering the practical trade-off analysis discussed in Section 3.7.

Second, no direct zeta-potential titrations were performed for the kaolin control suspensions or for the dose-dependent coagulant systems. Consequently, the electrostatic-destabilisation pathway hypothesised in Section 3.9 rests on indirect evidence (FTIR functional-group signatures and pH-response profiles) rather than direct surface-charge measurement. Similarly, no particle-size distribution or floc-size measurements were performed to characterise the aggregation kinetics.

Third, quantitative phytochemical characterisation of each coagulant was not performed. The FTIR spectra reported in Section 3.8 provide qualitative evidence of the presence of protein Amide bands, polysaccharide C–O–C bands, aromatic polyphenol bands, and species-specific markers (e.g., the juglone signature at 1508 cm^{-1} in Juglans regia), but do not quantify protein, total phenolics, polysaccharide, ash, or moisture content. The mechanistic hypothesis linking phytochemical class to coagulation pathway (Section 3.9) therefore remains a hypothesis consistent with the observed data rather than a demonstrated mechanistic model.

Fourth, no measurement of residual dissolved organic carbon (DOC), total organic carbon (TOC), or chemical oxygen demand (COD) was performed on the treated supernatants. Because plant-based coagulants introduce organic material by design, quantification of the residual organic load is an operationally essential parameter that should be measured before deployment recommendations can be made.

Fifth, comparison against conventional coagulants (alum, ferric chloride, and poly-aluminium chloride) relies on published values from independent studies rather than parallel testing under identical conditions in the present laboratory. Table 6 should therefore be interpreted as an indicative benchmark rather than as a statistically comparable dataset.

Sixth, no cost analysis, sludge quantification, or operational feasibility assessment was performed. The economic and operational competitiveness of leaf-based coagulants relative to conventional chemistries can therefore only be discussed qualitatively at this stage.

3.11 Recommendations for Future Work

The limitations enumerated in Section 3.10 define a clear and immediate research agenda for the follow-up phase of this study. Six priority activities are identified below, in approximate order of methodological urgency.

(1) Natural-water validation. Validation of the reported dose–pH–time regimes using natural water matrices — surface water (Tigris River, at both flood and baseline turbidity), local groundwater, and low-strength municipal wastewater — is a necessary and immediate next step. This will address the four confounding-

ACCEPTED MANUSCRIPT

factor concerns detailed in Section 3.10 and is the single most important prerequisite for translational deployment.

(2) Direct mechanistic characterisation. Zeta-potential titrations for kaolin controls (as a function of pH) and for dose–response curves of each coagulant will convert the electrostatic-destabilisation hypothesis (Section 3.9) into direct measurement. Complementary particle-size distribution and floc-size measurements via laser diffraction will characterise the aggregation process quantitatively.

(3) Quantitative phytochemical assays. Bradford, Folin–Ciocalteu, and phenol–sulphuric acid assays will quantify the protein, total phenolics, and polysaccharide contents of each coagulant, respectively; gravimetric ash and moisture determinations will complete the compositional profile. These quantitative data will confirm (or refute) the phytochemistry-informed species-selection framework proposed in Section 3.9.

(4) Parallel benchmarking against conventional coagulants. Jar-test experiments with alum, ferric chloride, and poly-aluminium chloride under identical kaolin/pH/dosage/settling-time conditions to the present study will replace the indicative-benchmark comparison of Table 6 with statistically comparable measurements.

(5) Techno-economic and sludge assessment. A full comparative cost analysis (leaf harvest, drying, milling, storage, coagulant preparation, acid/base dosing, sludge management, and post-treatment disinfection), together with sludge quantification (mass, dewaterability, loss on ignition, heavy-metal content), and an operational-feasibility assessment (power consumption for mixing, storage requirements, staffing needs) will convert the qualitative feasibility discussion of Section 3.7 into a deployment-oriented economic model.

(6) Advanced statistical optimisation and process modelling. The discrete-level factorial screening reported here identifies the operational envelope within which each species performs optimally. Response Surface Methodology (RSM), applied through central composite or Box–Behnken designs, will refine these optima into continuous response surfaces suitable for process-control applications. Salt-assisted extraction (with sodium chloride or calcium chloride) should also be investigated in this phase, as it has been reported to reduce optimal coagulant dosages by 30–50% in related plant-coagulant systems.

4. CONCLUSIONS

This study presents a first-stage empirical screening of five leaf-based natural coagulants — Morus alba, Vachellia nilotica, Trigonella foenum-graecum, Melia azedarach, and Juglans regia — for the removal of turbidity from synthetic kaolin water, under a full-factorial design spanning three pH levels, six coagulant dosages, and three settling times (N = 810 measurements). The four-way factorial ANOVA (adjusted $R^2 = 0.983$; all main effects and interactions significant at $p < 0.001$) confirmed that solution pH is the dominant operational factor ($\eta p^2 = 0.97$), followed by dosage ($\eta p^2 = 0.95$) and species ($\eta p^2 = 0.84$), settling time ($\eta p^2 = 0.83$). The highly significant three-way Species × pH × Dose interaction ($\eta p^2 = 0.85$) provides statistically consistent evidence for the phytochemistry-informed species-selection framework proposed on the basis of FTIR characterisation: each species presents a distinct pH-dose response profile consistent with its dominant phytochemical class (proteins/polyphenols, tannins, galactomannans, limonoids, and juglone-based naphthoquinones, respectively). Under mildly acidic conditions (pH 4), Morus alba achieved the highest single-species removal efficiency at 82.5 ± 0.8% (500 mg L^{-1}, 60 min settling), representing a 1.73-fold improvement over its neutral-pH optimum. This remains 8–13 percentage points below conventional inorganic coagulants, which achieve 90–95% at 12–25-fold lower doses (Table 6); leaf-based systems are therefore complementary rather than substitutive. Trigonella foenum-graecum showed the greatest pH sensitivity (loss of 81% removal capacity from pH 4 to pH 10), whereas Juglans regia showed the least pH sensitivity (loss of 56%) — a novel finding that suggests polysaccharide-rich species are best suited to acidic pre-treatment regimes, while species dominated by hydrophobic compounds provide the greatest operational robustness where acid dosing is not feasible. Even under the best condition identified (Morus alba, pH 4.0, 500 mg L^{-1}, 60 min settling), residual turbidity remained of the order of 90 NTU — well above the ≤ 5 NTU generally required for drinking water and was higher still at every other species optimum. Given also that no

ACCEPTED MANUSCRIPT

water-quality parameter other than turbidity was evaluated, leaf-based coagulation is best positioned as a decentralised first-stage turbidity-reduction step within a multi-barrier treatment train, rather than a stand-alone potable-water solution; downstream slow-sand filtration, disinfection and, where necessary, membrane polishing would be required for potable-quality output. The operational attractiveness of pH 4.0 pre-treatment is nonetheless conditional rather than categorical: acid demand scales with source-water alkalinity and treated water requires subsequent neutralisation, so the approach is most defensible for low-alkalinity waters and emergency or off-grid contexts.

ACKNOWLEDGEMENTS

The authors thank for the Department of Ecology College of Science, University of Basrah for laboratory facilities and technical assistance. This study was not funded by any public, private or not-for-profit agencies. The authors declare that they have no competing interests.

REFERENCES

Abujazar M.S.S., Karaağaç S.U., Abu Amr S.S., Alazaiza M.Y.D., Fatihah S. and Bashir M.J.K. (2022). Recent advancements in plant-based natural coagulant application in the water and wastewater coagulation-flocculation process: challenges and future perspectives. *Global NEST Journal*, *24*(4), 687-705.

Ahmad A., Kurniawan S.B., Abdullah S.R.S., Othman A.R. and Hasan H.A. (2022). Exploring the extraction methods for plant-based coagulants and their future approaches. *Science of the Total Environment*, *818*, 151668.

Alnawajha M.M., Abdullah S.R.S., Hasan H.A., Othman A.R. and Kurniawan S.B. (2024). Effectiveness of using water-extracted *Leucaena leucocephala* seeds as a coagulant for turbid water treatment: effects of dosage, pH, mixing speed, mixing time, and settling time. *Biomass Conversion and Biorefinery*, *14*, 11203-11216.

Ang W.L. and Mohammad A.W. (2020). State of the art and sustainability of natural coagulants in water and wastewater treatment. *Journal of Cleaner Production*, *262*, 121267.

Avornyo A.K., Hasan S.W., Banat F. and Chrysikopoulos C.V. (2024). Preparation, characterization, and applications of kaolin/kaolin-based composite membranes in oily wastewater treatment: recent developments, challenges, and opportunities. *Journal of Environmental Management*, *370*, 122800.

Benalia A., Derbal K., Amrouci Z., Baatache O., Khalfaoui A. and Pizzi A. (2024). Application of plant-based coagulants and their mechanisms in water treatment: a review. *Journal of Renewable Materials*, *12*(4), 667-698.

ACCEPTED MANUSCRIPT

575 Dotto J., Fagundes-Klen M.R., Veit M.T., Palácio S.M. and Bergamasco R. (2019). Performance of different
576 coagulants in the coagulation/flocculation process of textile wastewater. *Journal of Cleaner*
577 *Production*, *208*, 656-665.
578
579 El-Taweel R.M., Mohamed N., Alrefaey K.A., Husien S., Abdel-Aziz A.B., Salim A.I., Mostafa N.G., Said
580 L.A., Fahim I.S. and Radwan A.G. (2023). A review of coagulation explaining its definition,
581 mechanism, coagulant types, and optimization models; RSM, and ANN. *Current Research in Green*
582 *and Sustainable Chemistry*, *6*, 100358.
583
584 Hussain A. and Al-Baldawi I.A. (2025). Hybrid system using local plant as sustainable coagulation-
585 flocculation process. *Journal of Ecological Engineering*, *26*(1), 286-293.
586
587 Koul B., Bhat N., Abubakar M., Mishra M., Arukha A.P. and Yadav D. (2022). Application of natural
588 coagulants in water treatment: a sustainable alternative to chemicals. *Water*, *14*(22), 3751.
589 Kumar V., Al-Gheethi A., Asharuddin S.M. and Othman N. (2020). Potential of cassava peels as a sustainable
590 coagulant aid for institutional wastewater treatment: characterisation, optimisation and techno-
591 economic analysis. *Chemical Engineering Journal*, *420*, 127642.
592
593 Kurniawan S.B., Abdullah S.R.S., Imron M.F., Said N.S.M., Ismail N.I., Hasan H.A., Othman A.R. and
594 Purwanti I.F. (2020). Challenges and opportunities of biocoagulant/bioflocculant application for
595 drinking water and wastewater treatment and its potential for sludge recovery. *International Journal*
596 *of Environmental Research and Public Health*, *17*(24), 9312.
597
598 Lwasa A., Mdee O.J., Ntalikwa J.W. and Sadiki N. (2024). Performance analysis of plant-based coagulants in
599 water purification: a review. *Discover Water*, *4*(1), 108.
600 Maruthai S., Rajendran S., Selvanarayanan R. and Gowri S. (2025). Wastewater recycling
601 integration with IoT sensor vision for real-time monitoring and transforming polluted ponds into
602 clean ponds using HG-RNN. *Global NEST Journal*, *27*(4), 1-11.
603 Medic A., Zamljen T., Slatnar A., Hudina M. and Veberic R. (2021). Is juglone the only naphthoquinone in
604 *Juglans regia* L. with allelopathic effects? *Agriculture*, *11*(8), 784.
605
606 Muniz G.L., Borges A.C. and da Silva T.C.F. (2020). Performance of natural coagulants obtained from agro-
607 industrial wastes in dairy wastewater treatment using dissolved air flotation. *Journal of Water Process*
608 *Engineering*, *37*, 101453.
609 Mutar Z.H., Abdullah S.R.S. and Al-Baldawi I.A. (2025). Correlating the polysaccharide and protein contents
610 of five plant-derived coagulants with turbidity removal. *Journal of Ecological Engineering*, *26*(11),
611 231-241.
612 Naruka A.K., Suganya S., Senthil Kumar P., Amit C., Ankita K., Bhatt D. and Kumar M.A. (2021). Kinetic
613 modelling of high turbid water flocculation using native and surface functionalized coagulants
614 prepared from shed-leaves of *Avicennia marina* plants. *Chemosphere*, *272*, 129894.
615
616
617 Salem A.K., Almansoory A.F. and Al-Baldawi I.A. (2023). Potential plant leaves as sustainable green
618 coagulant for turbidity removal. *Heliyon*, *9*(5), e16278.
619 Sibiya N.P., Rathilal S. and Kweinor Tetteh E. (2021). Coagulation treatment of wastewater: kinetics and
620 natural coagulant evaluation. *Molecules*, *26*(3), 698.
621

ACCEPTED MANUSCRIPT

622 Venkatraman M., Rajendran S., Srinivasulu S. and Vijayakumar K. (2025). Water quality prediction and
623 classification using attention based deep differential RecurFlowNet with logistic giant armadillo
624 optimization. *Global NEST Journal*, *27*(1), 1-13.

625 Younis R.M. and Hasan S.M. (2026). Effect of temperature variation on the biological treatment of greywater
626 in the sequencing batch reactor. *Engineering and Technology Journal*, *44*(3), 1-18.

627

628 Zezulka Š., Maršálek B., Maršálková E., Odehnalová K., Pavlíková M. and Lamaczová A. (2024). Suspended
629 particles in water and energetically sustainable solutions of their removal—a review. *Processes*,
630 *12*(12), 2627.

631

632 Zurita F., Tejeda A., Ramirez-Ramirez A. and Montoya A. (2024). Integration of coagulation–flocculation
633 (with natural coagulant) to constructed wetlands for color removal from tequila vinasses. *Water*,
634 *16*(21), 3151.

635

ACCEPTED MANUSCRIPT